

## DC CONDUCTIVITY AND CHARGE TRANSPORT IN VITREOUS $\text{As}_2\text{S}_3\text{Ge}_8 - \text{Te}$ FILMS

M. CIOBANU\*, D. TSIULYANU

*Department of Physics, Technical University of Moldova, bd. Dacia 41, Chisinau 2060, Moldova*

Amorphous tellurium and Te based quaternary films have been grown onto both glassy (Pyrex) and ceramic  $\text{Al}_2\text{O}_3$  substrates by a high speed thermal deposition in vacuum. The SEM and XRD analysis of the films was provided and the DC conductivity was studied in order to elucidate the influence of Te concentration on mechanisms of charge transport. It was shown that both material composition and substrate influence the phase-state structure of the films, which results in a strong variation of their parameters and electrical properties. The electrical conductivity is shown to be realized by either charge transport via extended states or hopping via localized states in valence band tail, dependently on the film composition and temperature regime.

(Received September 30, 2017; Accepted January 6, 2018)

*Keywords:*  $\text{As}_2\text{S}_3\text{Ge}_8 - \text{Te}$ , DC measurements, Transport mechanisms

### 1. Introduction

Chalcogenide glassy semiconductors (ChGS) have become attractive by their application properties caused by the effects of either threshold (ovonic) switching or memory [1-3]. In recent years, these semiconductor materials draw attention due to phenomena of their effective and stable interaction with ambient gases [4-8]. In order to elucidate the cause of these phenomena and eventually to advance the applicative performances of the quaternary ChGS in the above - mentioned purposes, it is necessary estimation of both parameters of the energy spectrum of the material in question and the mechanism of the electric charge transport therein. It is well known that the current flow in glassy chalcogenides is controlled by competition of three mechanisms of charge transport via: a) non localized (extended) states above mobility edges; b) tails of localized states close to mobility edges and c) localized states near the middle of the mobility gap, where the Fermi level is pinned [9-11]. The last two mechanisms are related by phonon assisted hopping between localized states. Investigation of temperature dependent DC conductivity allows distinguishing between these mechanisms of charge transport and to determine the predominant mechanism under given conditions, because the activating energy for the above mentioned transport mechanisms is essentially different. The present paper is devoted to study the mechanisms of current transport in quaternary  $\text{As}_2\text{Ge}_8\text{S}_3 - \text{Te}$  films, along with films of pure amorphous Te, for comparison.

### 2. Materials and methods

The chalcogenide thin films have been prepared by thermal “flash” evaporation of previously synthesized materials  $\text{As}_2\text{Te}_{13}\text{Ge}_8\text{S}_3$  and  $\text{As}_2\text{Te}_{130}\text{Ge}_8\text{S}_3$ , as well as of polycrystalline Te, from tantalum boat, onto glass (Pyrex) or ceramic  $\text{Al}_2\text{O}_3$  substrates at a working pressure of  $10^{-5}$  Torr. The growth velocity of the film was in the order of 30 nm/s, and the area of deposition around 15 mm<sup>2</sup> for films grown on Pyrex substrates and 5 mm<sup>2</sup> for those grown on sintered alumina substrates. The surface morphology of the films was made visible with a VEGA TESCAN TS 5130 MM scanning electron microscope at an acceleration voltage of 30 kV, but their

---

\*Corresponding author: marina.ciobanu@fiz.utm.md

thickness, being around 60 nm, was determined using the optical microinterferometer MII - 4. The structural investigations of the grown films were carried out by the X-ray analyses using the DRON -YM1 diffractometer by  $FeK_{\alpha}$  radiation. Rotation velocity of the scintillation counter was 2 (or / and 4) angle degrees /min.

DC conductivity measurements were carried out using the chalcogenide films grown both on Pyrex and sintered alumina substrates. The contacts used for DC measurements should be ohmic (i.e. invisible) such that the DC current flowing through the sample for a fixed intensity of external electric field is determined only by the transport parameters of the material. To realize the ohmic contacts for chalcogenide films in question, a number of electrodes (gold, platinum, different silver pastes) have been tested. The measurements of current - voltage ( I / V ) characteristics of thin films provided with different electrodes have allowed outlining the most suitable of them, and namely, either the symmetric Ag - Ag contacts prepared from paste „Kontaktol” (Keller chemical science & production, Russia) or the symmetric Pt - Pt contacts grown using the cathodic scattering. These pairs of electrodes exhibit nearly the same behavior. Thus, for the films grown on Pyrex substrates, the electrodes have been painted over film surface using the silver paste „Kontaktol” at the distance of ~ 4,5 mm, which were connected in circuit by means of copper wires. The films grown onto ceramic  $Al_2O_3$  substrates were contained the previously deposited platinum interdigital electrodes with an electrode width of 15  $\mu m$  and interelectrode distances of 45  $\mu m$ . The last mentioned films were encapsulated in standard TO - 16 sockets and their contacts were thermally bonded to socket pins by means of copper wires.

The thin film devices were put onto an electrical refrigerator allowing cooling the sample until 10<sup>0</sup> C. Then, these two pieces were put together in an electric furnace for heating and regulating the working temperature of the film. A platinum resistance temperature detector PT - 100 close to the film has been used for assisting the temperature control. The current - voltage characteristics have been carried out at different temperatures in normal air ambient conditions. The data acquisition and processing was performed with PC and a interface board AT-MIO-16X manufactured by National Instruments Inc., but the electrometer Y5-11 has been used as a I / V converter. In all cases the applied voltage was varied between -5V and +5V with a step of 20 mV and the respective values of the current were measured. Delay time between measurements was 2s. The measurements were performed at temperatures between 10 - 200<sup>0</sup>C.

### 3. Results and discussion

#### 3.1. The surface morphology and phase-state structure

Figs. 1 and 2 shows the SEM images of the quaternary  $As_2Te_{13}Ge_8S_3$  and  $As_2Te_{130}Ge_8S_3$  chalcogenides along with films of elemental Te, grown on different substrates, using the same (~30 nm/s) deposition rate. As can be seen the films grown on glassy (Pyrex) substrates are continuous layers, but the films grown on sintered alumina consists of agglomerated islands, resulting in the films with great surface roughness. In all cases no crystallite tracks are observed.

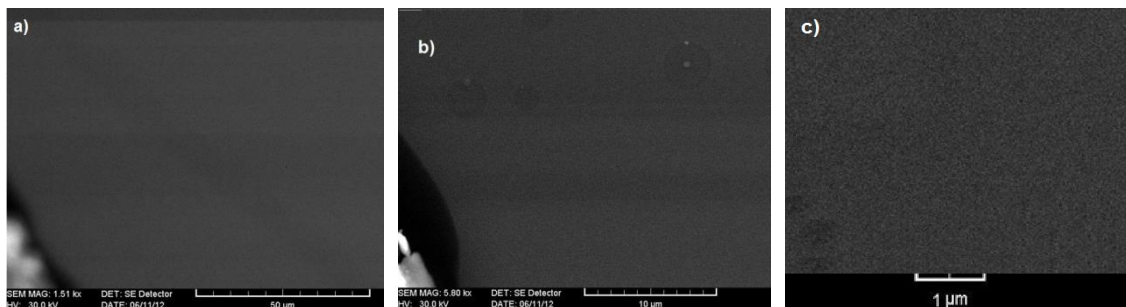


Fig. 1. SEM micrographs of (a)  $As_2Te_{130}Ge_8S_3$ , (b)  $As_2Te_{13}Ge_8S_3$  and (c) pure Te films grown on Pyrex substrates.

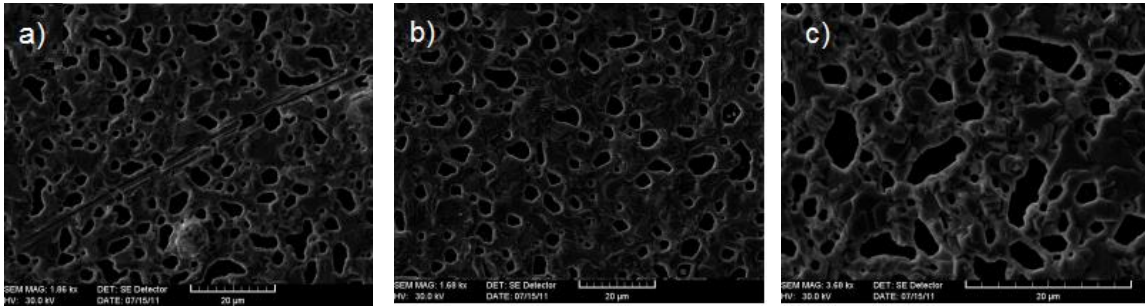


Fig. 2. SEM micrographs of (a)  $As_2Te_{130}Ge_8S_3$ , (b)  $As_2Te_{13}Ge_8S_3$  and (c) pure Te films grown on sintered alumina ( $Al_2O_3$ ) substrates

Fig. 3 shows the XRD patterns of quaternary  $As_2Te_{13}Ge_8S_3$ ,  $As_2Te_{130}Ge_8S_3$  and pure Te, films deposited on Pyrex substrates. It is seen that the films with enhanced (91at.%) concentration of Te (Fig.3a) contains the diffraction peaks, which indicate the existence of crystalline phase of it. Nevertheless, no peaks of crystalline Te are observed in both  $As_2Te_{13}Ge_8S_3$ , and pure tellurium films, that is these films are in the vitreous state.

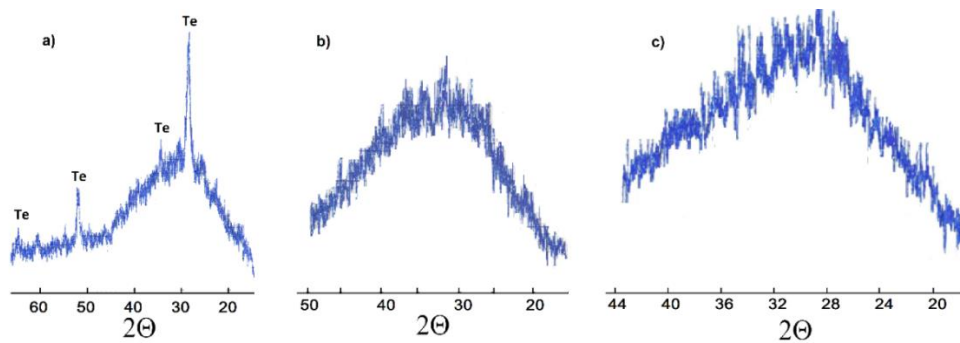


Fig. 3. XRD diffraction pattern of (a)  $As_2Te_{130}Ge_8S_3$ , (b)  $As_2Te_{13}Ge_8S_3$  and (c) pure Te films grown on Pyrex substrate

The XRD patterns of quaternary  $As_2Te_{13}Ge_8S_3$ ,  $As_2Te_{130}Ge_8S_3$  and pure Te, films deposited on alumina substrates are shown in Fig. 4. It is evident that the  $As_2Te_{13}Ge_8S_3$  films (Fig.4b) are in the amorphous state. The quaternary  $As_2Te_{130}Ge_8S_3$  films with higher concentration of tellurium, as well as pure Te films show very small peaks corresponding to crystalline phases of Te (Figs. 4 a, c) indicating their nearly amorphous nature. No peaks corresponding to oxides of tellurium are visible in the XRD patterns. These results are in agreement with SEM observation

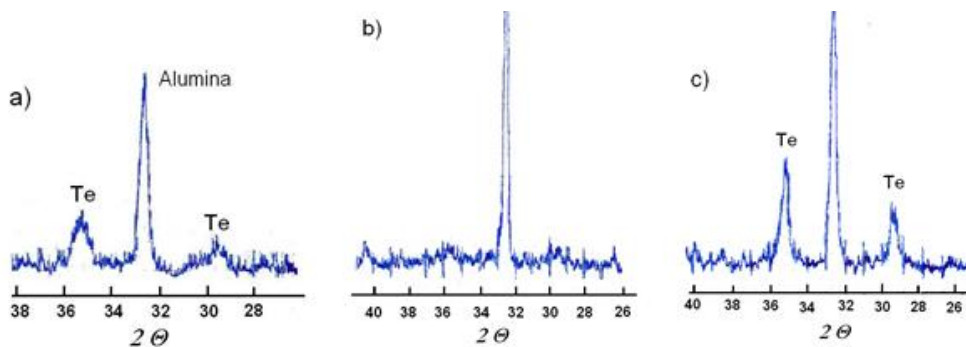


Fig. 4. XRD diffraction pattern of (a)  $As_2Te_{130}Ge_8S_3$ , (b)  $As_2Te_{13}Ge_8S_3$  and (c) pure Te films grown on sintered alumina ( $Al_2O_3$ ) substrates

### 3.2. DC conductivity and contacts

The investigation of temperature dependence of the dark DC conductivity in disordered systems allows obtaining the information concerning the fundamental parameters of the material, such as the mobility gap, the minimum metallic conductivity, the density of localized states at the Fermi level, close to the middle of mobility gap, etc., which control the transport mechanisms. An important role in these measurements plays the contact. The contacts used for DC measurements in this work, were thoroughly chosen to be ohmic as the DC current flowing through the sample for a fixed external field must be determined by the charge transport parameters of the chalcogenide film only. As have been mentioned above, the symmetric Ag – Ag contacts prepared from paste „Kontaktol” and Pt – Pt contacts, grown via cathodic scattering exhibit nearly ohmic behavior and namely this kind of contacts have been used in our experiments. Figure 5 (a) shows the typical I / U characteristics of  $\text{As}_2\text{Te}_{13}\text{Ge}_8\text{S}_3$  based films with symmetric Ag electrodes at different temperatures. In all cases the I / U characteristics are linear and follow the Ohm's law. The similar characteristics have been obtained for both  $\text{As}_2\text{Te}_{130}\text{Ge}_8\text{S}_3$  and pure Te films.

Using these data, the temperature dependence of conductivity has been highlighted for all compositions of ChGS in question. The results obtained for  $\text{As}_2\text{Te}_{13}\text{Ge}_8\text{S}_3$  films are shown in Figure 5 (b), where  $\ln \sigma$  is plotted as a function of  $10^3/T$ . The obtained curve consists of two straight lines with different slopes, which gives evidence that the charge transport occurs by different mechanisms. According to this curve, the conductivity of the film can be expressed as sum of two terms, each of them controlling the current transport by different temperature regimes:

$$\sigma = C_1 \exp\left(-\frac{E_1}{kT}\right) + C_2 \exp\left(-\frac{E_2}{kT}\right) \quad (1)$$

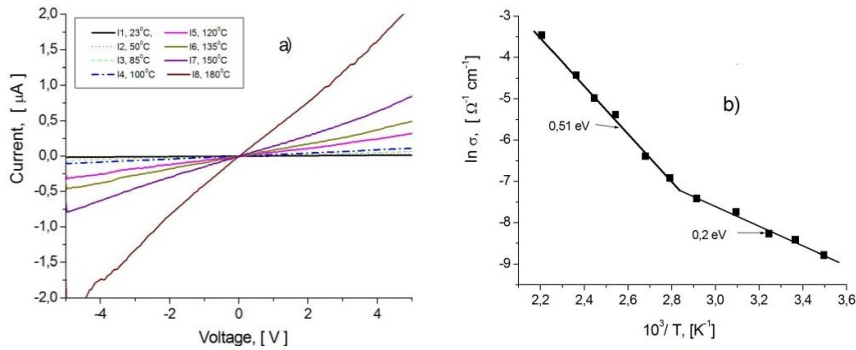


Fig. 5. a) I-U characteristics and b)  $\ln \sigma$  versus reciprocal temperature of amorphous  $\text{As}_2\text{Te}_{13}\text{Ge}_8\text{S}_3$  films.

Following the Mott and Davis model of the density of states [9] the first term controls the high temperature conductivity and is due to charge (holes) transport via non localized (extended) states close to the mobility edge, but the activation energy  $E_1$  means the position of Fermi level relative to mobility edge of the valence band. The experimental values of  $E_1$  and  $C_1$ , calculated

from both, the slope of the first line and its extrapolation to  $\frac{10^3}{T} = 0$  are given in Table 1.

Table 1. Semiconducting parameters of  $As_2S_3Ge_8Te_x$  films related to transport mechanisms.

Transport mechanism	Composition , (x)	$C_1$ $\Omega^{-1} cm^{-1}$	$C_2$ $\Omega^{-1} cm^{-1}$	$E_1, eV$	$E_2, eV$	$E_g, eV$	$\sigma_{min}$ $\Omega^{-1} cm^{-1}$
Extended states	1	1		$\sim 0,18$		$\sim 0,36$	1
	13	$\sim 10^4$		0,51		$\sim 1,0$	$10^3$
	130	$\sim 140$		$\sim 0,2$		$\sim 0,4$	14
Hopping via localized states	13		0,61		0,2		
	130				0,05		

As the pre-exponential term is given as  $C_1 = \sigma_{min} \exp(\frac{\gamma}{k})$  [9], where  $\gamma$  is the temperature coefficient of the optical gap, the minimal metallic conductivity could be assessed. Taking  $\gamma = 2 \cdot 10^{-4} eV/degree$  [12] we have obtained  $\sigma_{min} \approx 10^3 \Omega^{-1} cm^{-1}$  (Table 1). The second term in relation (1) is due to phonon assisted hopping between the localized states of band tiles. In this case, the activation energy is  $E_2 = E_F - E_B + W_1$ , where  $E_F - E_B$  is the energetic distance between the edge of the valence band tail and Fermi level, but the  $W_1$  is the hopping energy.

The temperature dependence of DC conductivity for Te enriched composition  $As_2Te_{130}Ge_8S_3$  is shown in Fig. 6 along with data for pure tellurium films for comparison.

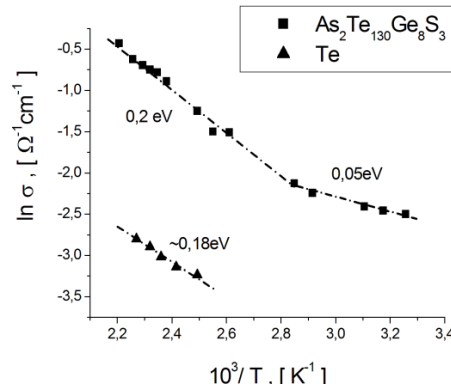


Fig. 6. Temperature dependence of DC conductivity of  $As_2Te_{130}Ge_8S_3$  and Te films.

Again the curve consists of two straight lines with different slopes, but both the position and slopes are essential different than for  $As_2Te_{13}Ge_8S_3$  films. The estimated values of minimum metallic conductivity and mobility gap for both  $As_2Te_{130}Ge_8S_3$  and pure Te films are also listed in Table 1. Note, that the value of the gap  $E_g \approx 0,36 eV$  for amorphous Te is in a good agreement with results obtained early by other authors [13].

#### 4. Conclusions

Amorphous quaternary  $As_2Ge_8S_3$ -Te and pure Te films can be grown onto both glassy (Pyres) and sintered alumina substrates via a high speed thermal deposition in vacuum. Structure, parameters and electrical properties of the films depend on material composition and nature of substrates. The width of mobility gap and minimal metallic conductivity of the films decrease with Te concentration increase, from  $E_g = 1,0 eV$  ( $\sigma_{min} \approx 10^3 \Omega^{-1} cm^{-1}$ ) for  $As_2Te_{13}Ge_8S_3$  to  $E_g = 0,36 eV$  ( $\sigma_{min} \approx 1 \Omega^{-1} cm^{-1}$ ) for pure amorphous Te. At room temperature, the electrical conductivity of the films is realized via extended states, being minimal  $\sigma \approx 2 \cdot 10^{-4} \Omega^{-1} cm^{-1}$  for

As<sub>2</sub>Te<sub>13</sub>Ge<sub>8</sub>S<sub>3</sub>. At lower temperature, the charge transport occurs by hopping via localized states in the valence band tails.

### Acknowledgements

This work was financially supported by Technical University of Moldova through Institutional Grant 15.817.02.29A. The authors wish to thank Dr. M. Enache from NCMST of TUM for SEM analysis and Dr. G. F. Volodina from IAP ASM for XRD analysis.

### References

- [1] S.R. Ovshinsky, Phys.Rev. Lett. **21**, 1450 (1968).
- [2] S.R. Ovshinsky, H.Fritzsche,IEEE Trans. Elect. Dev. **ED-209**, 91 (1973).
- [3] I. Stratan, Thesis doct.sci.,*cc.sibimol. bnrm. md / opac/bibliographic View/333088*, Chisinau, 107, 2011.
- [4] K. Koleva, C. Popov, T. Petkova, P. Petkov, I. N. Mihailescu, J - P Reithmaier, Sens. Actuators B **143**, 395 (2009).
- [5] J. Wüsten, K. Potje-Kamloth, Sens.Actuators B **145**, 216 (2010).
- [6] M. Ciobanu, Meridian Ingineresc **3**, 58 (2015).
- [7] D. Tsiulyanu, M. Ciobanu, Proc. of 3<sup>rd</sup> ICNBE Chisinau 2015, Springer **55**, 382 (2016).
- [8] D.Tsiulyanu, M. Ciobanu, Sens. Actuators B **223**, 95 (2016).
- [9] N. F. Mott and E.A. Davis, //Electron processes in non-crystalline materials//, Clarendon Press, Oxford, (1979).
- [10] P. Nagels, Electronic transport phenomena in amorphous Semiconductors ( in: Amorphous Semiconductors, Ed. M.H. Brodsky), Springer (1979).
- [11] M. Popescu, A. Andriesh, V. Chumach, M. Iovu, S. Shutov, D. Tsiuleanu, //Fizica sticlelor calcogenice//, Ed. Stiintifică I.E.P. Stiinta, Bucuresti –Chisinau(1996)
- [12] A.M. Andriesh, D.I Tsiulyanu, Phys. Stat. Sol. (a) **19** 307 (1973).
- [13] A.K. Ray, R.Swan, C.A.Hogarth, J.Non-Cryst. Solids **168**,150 (1994).